N·H

Temperature dependence of the fast, near-band-edge scintillation from CuI, HgI$_2$, PbI$_2$, ZnO:Ga, and CdS:In

Stephen E. Derenzo[a], Marvin J. Weber[a], Mattias K. Klintenberg[a,b]

[a]*Lawrence Berkeley Laboratory,University of California, Berkeley, CA 94720, U.S.A*

[b]*Department of Physics, Uppsala Univeristy, Uppsala, Sweden*

Abstract

We present temperature-dependent pulsed x-ray data on the decay time spectra, wavelengths, and intensities of fast (ns) radiative recombination in five direct, wide-bandgap semiconductors: CuI, HgI$_2$, PbI$_2$, and n-doped ZnO:Ga and CdS:In. At 12K the luminosity of powder samples is 0.30, 1.6, 0.40, 2.0, and 0.15, respectively, relative to that of BGO powder at room temperature. Increasing the temperature of CuI to 346K decreases the luminosity by a factor of 300 while decreasing the fwhm of the decay time spectra from 0.20 ns to 0.11 ns. Increasing the temperature of HgI$_2$ to 102K decreases the luminosity by a factor of 53 while decreasing the fwhm from 1.6 ns to 0.5 ns. Increasing the temperature of PbI$_2$ to 165K decreases the luminosity by a factor of 27 while decreasing the fwhm from 0.52 ns to 0.15 ns. Increasing the temperature of ZnO:Ga to 365K decreases the luminosity by a factor of 33 while decreasing the fwhm from 0.41 ns to 0.21 ns. Increasing the temperature of CdS:In to 295K decreases the luminosity by a factor of 30 while decreasing the fwhm from 0.20 ns to 0.17 ns. All emission wavelengths are near the band edge. The luminosities decrease much faster than the radiative lifetimes, therefore the reduction in luminosity is not primarily due to thermal quenching of the excited states but mostly due to thermally activated trapping charge carriers on nonradiative recombination centers. Since the radiative and nonradiative processes occur on different centers, increasing the ratio of radiative to nonradiative centers could result in a class of inorganic scintillators whose decay time and radiative efficiency would approach fundamental limits (i.e. <1 ns and 100,000 photons per MeV).

1. Introduction

Commonly used inorganic scintillators are, in many cases, either slow or have low radiative efficiency. For example, NaI:Tl, CsI:Tl, and Bi$_4$Ge$_3$O$_{12}$ are relatively efficient, but have long decay times (>200 ns) because their transitions are spin forbidden. The core-valence luminescence of BaF$_2$ is fast but has a low radiative efficiency (<2,000 photons per MeV) due to the low probability of forming holes in an upper core band. Currently, the inorganic scintillators with the best combination of speed and effi-

ciency are Ce-doped, but their radiative decay times are limited to ~10-60 ns due to the limited overlap of the 5d and 4f electronic orbitals. In this paper, we explore five direct wide-bandgap semiconductors, a neglected class of scintillators that provide the possibility of bright, sub-ns emission. The availability of such scintillators containing high proportions of atoms chosen for the efficient detection of particular ionizing radiation (e.g. x-rays, gamma rays, neutrons) would substantially improve instrumentation for nuclear physics, high energy physics, and medical imaging.

2. Fast, near-band-edge emission from direct gap semiconductors

Whereas compound semiconductors have been used extensively for conductivity radiation detectors (see, for example, ref. [1]), several of these materials also have fast near-band-edge emission that is potentially of interest for scintillation. In contrast with commonly used ionic scintillators, near-band-edge emitting semiconductors have excited states that extend over many atoms and this involves negligible lattice relaxation. This emission may arise from band-to-band or free exciton recombination transitions. If the transition is direct and parity allowed, the radiative lifetime may be short, a nanosecond or less. Practical semiconducting crystals contain numerous defects and impurities that give rise to nonradiative recombination centers as well as free-to-bound, donor-acceptor pair, and bound exciton radiative transitions [2]. Consequently, the radiative efficiencies and decay times can vary from sample to sample.

An example of intentional doping to enhance fast, near-band-edge emission is the work of Lehmann on the direct semiconductors ZnO and CdS [3,4]. He showed in the mid-1960s that quenching could be reduced by n-doping these materials with Ga and In, respectively, and preparing them under reducing conditions. Scintillation from semiconductors has also been demonstrated by doping them with isovalent impurities. In the cases of CdS:Te [5] and ZnSe:Te [6], however, the lattice relaxation about the excited centers yields red-shifted emission and slower radiative decay rates.

3. Experimental measurements of luminosity and decay time

We have examined the temperature dependence of the fast, near-band-edge emission from three undoped and two doping semiconductors.

3.1. Materials

The CuI, PbI_2, and HgI_2 powders were purchased from Strem Chemicals with a metals purity > 99.999%. The ZnO:Ga(0.3%) and CdS:In(0.1%) powders were prepared by T. Perry of the Lawrence Livermore National Laboratory in collaboration with W. Lehmann. The powders were contained in fused silica cuvettes for measurements.

3.2. Pulsed x-ray system

This system, described more fully in reference [7], consists of an ultrafast laser system that delivers sub-ps pulses of 400-nm light onto the photocathode of a light-excited x-ray tube. Photoelectrons are accelerated to a tungsten anode at +30 kV to produce 35 ps (fwhm) pulses of x-rays with a mean energy of 18 keV [8]. Fluorescent photons from the sample are detected by a microchannel phototube with 35 ps (fwhm) response. The samples were cooled with an Advanced Research Systems, Inc. ARS2-A closed-cycle helium refrigerator.

Figure 1 shows the overall system impulse response, determined by using a 1-mm thick PbF_2 crystal, painted black on five sides. In this material, recoil photoelectrons produce prompt bremsstrahlung radiation that is peaked at the low end of the photon energy spectrum. A small amount of fluorescence is also observed with a decay time of 28 ns and this component is not used in the impulse response.

3.3. Fitting Procedures

To determine exponential decay times and fractions, the impulse response function was convolved with a sum of 30 components and their decay times a fractions were varied to minimize a log likelihood fit to the data [7]. Each of the decay times was constrained to lie within a narrow band and all fractions were constrained to be non-negative.
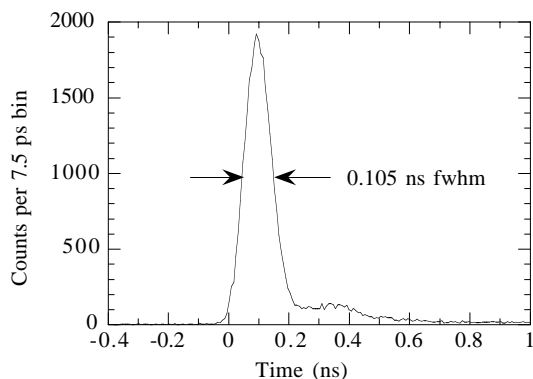
Figure 1. Impulse response from a thin PbF_2 crystal painted black on five sides.

Figure 2. Decay time spectra for CuI at four temperatures.

Table 1 Luminosity and principal fast decay times for CuI

Band edge	12K	99K	293K	346K
Luminosity	0.30	0.12	0.02	0.0013
fwhm (ns)	0.20	0.20	0.25	0.11
Component 1	0.12 ns 58%	0.10 ns 56%	0.13 ns 28%	<0.05 ns 70%
Component 2	0.28 ns 26%	0.29 ns 13%	0.27 ns 62%	0.13 ns 2%
Component 3	1.4 ns 7%	1.1 ns 9%	1.1 ns 5%	0.7 ns 1%

4. Results

In the typical case of a sample with a luminosity comparable to that of room temperature BGO, two million events were recorded in one hour. The luminosities and decay times/percentages are only accurate to about 20% of their value due to variability in sample placement and the well-known difficulty of fitting sums of exponentials to data. In the tables to follow, the luminosity is given relative to that of BGO powder at 295K and is reported only for components with decay times <1 µs.

4.1. Measurements of CuI

The emission spectrum of CuI (density 5.67 g/cm^3, bandgap 3.1 eV at 4K) consists of weak, near-edge exciton bands and broad bands attributed to radiative recombination at lattice defects, the most intense of which occurs at ~420-430 nm. There is a redistribution of intensities in the bands with increasing temperature, however the free exciton band is observed up to 400 K [9].

Figure 2 shows the decay time spectra for CuI at four temperatures; table 1 lists the results of the fits to the data.
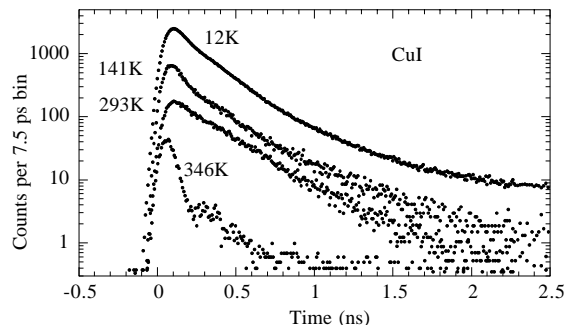
4.2. Measurements of HgI$_2$

The luminescence spectrum of tetragonal (red) mercuric iodide at 4 K (density 6.28 g/cm^3, bandgap 2.37 eV) consists principally of two bands: an exciton band at 2.33 eV and a featureless impurity/defect band at 2.22 eV. The latter band has been attributed to traps associated with iodine vacancies [10] and, more recently, to exciton annihilation at mercury vacancies [11]. Anderson has reported that the exciton-polariton decay rate decreases precipitously with increasing temperature [12]. The defect band luminescence exhibits a rapid rise time; the related formation rate is largely temperature independent and greater than the exciton decay rate. With increasing temperature the decay rates of the two bands become comparable. Nonradiative decay dominates at temperatures > 100K. Scintillation in HgI$_2$ has been reported briefly [13].

Figure 3 shows the decay time spectra for HgI$_2$ at four temperatures; table 2 lists the results of the fits to the data.
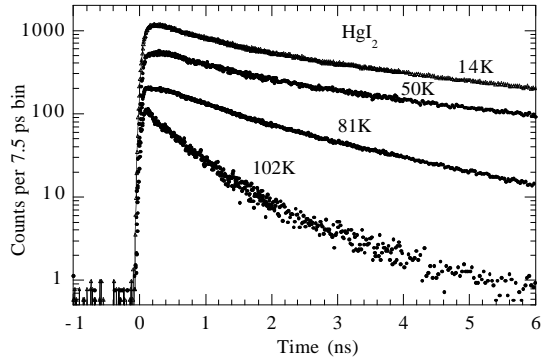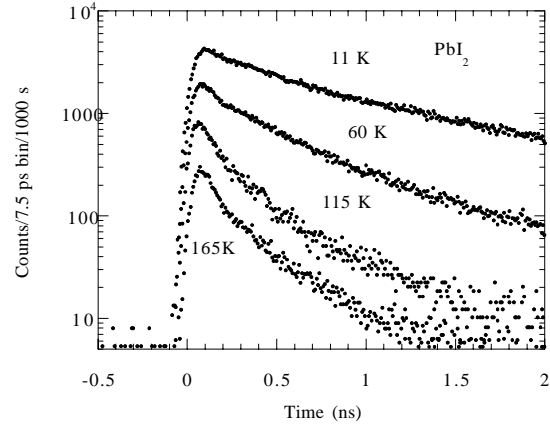
Figure 3. Decay time spectra of HgI$_2$ at four temperatures.

Table 2 Luminosity and principal fast decay times for HgI$_2$

	14K	50K	81K	102K
Luminosity	1.6	0.80	0.18	0.03
fwhm	1.6 ns	1.5 ns	1.2 ns	0.5 ns
Component 1	0.6 ns	0.8 ns	0.75 ns	0.50 ns
	9%	10%	14%	48%
Component 2	2.0 ns	2.3 ns	1.7 ns	1.2 ns
	22%	22%	45%	34%
Slow Components	> 5 ns	> 5 ns	> 5 ns	> 5 ns
	70%	68%	40%	17%

4.3. Measurements of PbI$_2$

Th emission spectrum of PbI$_2$ at low temperatures (density 6.16 g/cm^3, bandgap 2.55 eV) consists of near-edge lines due to free and bound excitons and broad overlapping bands shifted by ~100-200 meV attributed to donor-acceptor pair transitions [14-16].

Figure 4 shows the decay time spectra for PbI$_2$ at four temperatures; table 3 lists the results of the fits to the data.

Figure 4. Decay time spectra of PbI$_2$ at four temperatures.

Table 3 Luminosity and principal fast decay times for PbI$_2$

Band edge	11K	60K	115K	165K
Luminosity	0.40	0.10	0.025	0.015
fwhm	0.52 ns	0.32 ns	0.16 ns	0.15 ns
Component 1	0.16 ns	0.16 ns	0.11 ns	0.06 ns
	10%	24%	50%	35%
Component 2	0.58 ns	0.43 ns	0.40 ns	0.29 ns
	25%	38%	24%	21%
Component 3	1.8 ns	1.3 ns	1.4 ns	1.4 ns
	43%	29%	10%	11%

4.4. Measurements of ZnO:Ga

The introduction of ~0.3% Ga into ZnO (density 5.61 g/cm^3, bandgap 3.44 eV at 4K) introduces a degenerate donor band overlapping the bottom of the conduction band and increases the conductivity of the material. The edge emission spectrum at low temperatures reflects the density of states; at room temperature it is a broad band extending from ~3.1 to 3.3 eV [4].

Figure 5 shows the decay time spectra for ZnO:Ga at four temperatures; table 4 lists the results of the fits to the data.
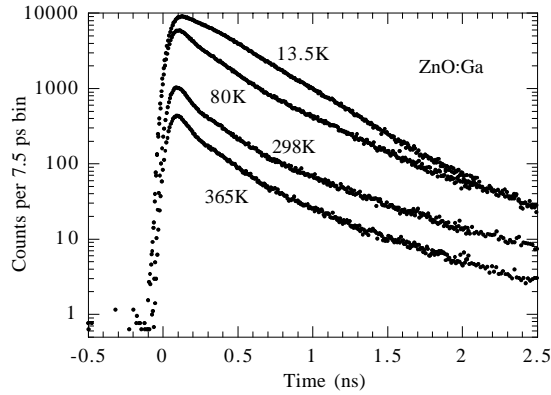
Figure 5. Decay time spectra of ZnO:Ga at four temperatures.

Table 4 Luminosity and principal fast decay times for ZnO:Ga

	13.5K	80K	295K	365K
Luminosity	2.0	1.0	0.15	0.06
fwhm (ns)	0.41	0.27	0.21	0.21 ns
Component 1		0.14 ns 45%	0.11 ns 39%	0.11 ns 37%
Component 2	0.30 ns 80%	0.35 ns 17%	0.32 ns 23%	0.29 ns 23%
Component 3	0.54 ns 18%	0.60 ns 32%	0.82 ns 30%	0.78 ns 28%

4.5. Measurements of CdS:In

At high doping levels, the conduction band of CdS:In (density 4.83 g/cm^3, bandgap 2.58 eV) is degenerate and partly filled with donor electrons. Emission is due to non-*k*-conserving band-to-band transitions [17, 18]. The width and peak wavelength of the band change with changing In concentration [4]. At 0.1% In the edge emission spectrum at room temperature is a featureless band that extends from ~2.2 to 2.5 eV.

Figure 6 shows the decay time spectra for CdS:In at four temperatures; table 5 lists the results of the fits to the data.

5. Discussion

Because we are interested in the total luminosity change with temperature, no spectral filtering was
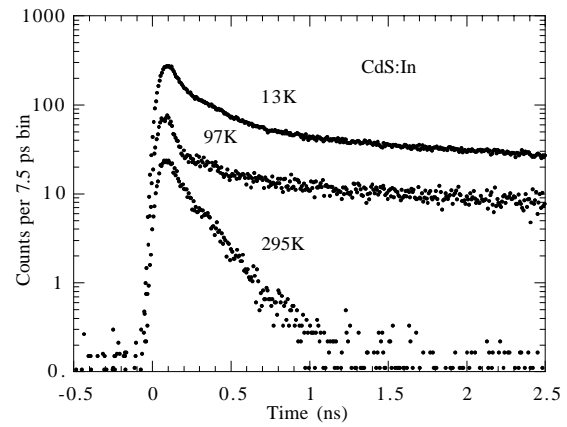

Figure 6. Decay time spectra of CdS:In at three temperatures.

Table 5 Luminosity and principal fast decay times for CdS:In

	13K	97K	295K
Luminosity	0.13	0.035	0.001
fwhm (ns)	0.20	0.14	0.17
Component 1	0.10 ns 13%	0.31 ns 8%	0.12 ns 95%
Component 2	1.2 ns 11%	0.73 ns 7%	2.2 ns 4%
Component 3	7 ns 43%	6 ns 43%	
Component 4	21 ns 32%	21 ns 43%	

used in obtaining the above results. Thus the observed scintillation at low temperatures may involve free and bound exciton emission, free-to-bound carrier emission, and donor-acceptor pair transitions.

A characteristic immediately evident in the above results is that at all but the highest temperatures, increasing the temperature results in large changes in sample luminosity but only small changes in decay time(s). This is in contrast to normal thermal quenching where increasing the temperature decreases both the luminosity and decay time at the same rate. From this we conclude that (1) the number of radiative excited states is controlled by the temperature and the activation energy for competitive trapping of charge carriers on nonradiative centers, and (2) the radiative excited states, once formed, are not subject to quenching. The luminosity vs.

temperature data reveal the existence of one or more activation energies for nonradiative trapping in the range of tens to hundreds of meV.

At the highest temperatures, the decay time begins to decrease. A similar luminosity and decay time behavior has also been reported for GaN [19, 20], and attributed to thermal detrapping of holes from acceptor atoms.

The observed luminosities at low temperatures are comparable to that of BGO at 295K (8200 photons/MeV) and thus are much less than expected if there were no initial nonradiative recombination or trapping of charge carriers. Nevertheless, the present materials are potentially useful scintillators at low temperatures. To improve efficiency and make possible higher temperature operation, one needs to reduce the number of nonradiative recombination centers and/or introduce acceptor levels such that the probability of radiative transitions to these levels is more competitive with nonradiative recombination rates. This would result in fast, bright scintillation.

Acknowledgments

References

[1]   D. S. McGregor and H. Hermon, "Room-temperature compound semiconductor radiation detectors," *Nucl. Instr. and Meth. A* vol. 395, pp. 101-124. 1997).

[2]   P.Y. Yu and M. Cardona, *Fundamentals of Semiconductors*, 3rd edition (Springer, Berlin, 2001), pp.345-369.

[3]   W. Lehmann, "Optical absorption edges of ZnO and CdS," *J Electrochem Soc,* vol. 112, pp. 1150-1151, 1965.

[4]   W. Lehmann, "Edge emission of n-type conducting ZnO and CdS," *Solid-State Electronics,* vol. 9, pp. 1107-1110, 1966.

[5]   P. Schotanus, P. Dorenbos and V. D. Ryzhikov, "Detection of CdS(Te) and ZnSe(Te) scintillation light with silicon photodiodes," *IEEE Trans Nucl Sci,* vol. NS-39, pp. 546- 550, 1992.

[6]   V. Ryzhikov, N. Starzhinsky, L. Gal'chinetskii, et al., New semiconductor scintillators ZnSe (Te,O) and integrated radiation detectors based thereon, *IEEE Trans Nucl Sci,* vol. 48, pp. 356-359, 2001..

[7]   S. E. Derenzo, M. J. Weber, W. W. Moses, et al., "Measurements of the intrinsic rise times of common inorganic scintillators.," *IEEE Trans Nucl Sci,* vol. NS-47, pp. 860-864, 2000.

[8]   S. C. Blankespoor, S. E. Derenzo, W. W. Moses, et al., "Characterization of a pulsed X-ray source for fluorescent lifetime measurements," *IEEE Trans Nucl Sci,* vol. NS-41, pp 698-702, 1994.

[9]   V. A. Nikitenov, V. I. Popolitov, S. G. Stoyukhin, et al., Growth and optical properties of CuI single crystals, *Sov. Tech. Phys. Lett*., vol. 5, pp. 493-495, 1979.

[10] J. L. Merz, Z. L. Wu, L. Van Den Berg, et al., "Low temperature photoluminescence of detector-grade HgI_2", *Nucl. Instr. and Meth.,* vol. 213, pp. 51-64, 1983.

[11] I. Kh. Akopyan, B. V. Bondarenko, O. N. Volkova, et al., "Luminescence of mercuric iodide crystals", *Phys. Solid State*, vol. 39, pp. 58-63, 1997.

[12] R. J. M. Anderson, Decay dynamics of free and trapped excitons in tetragonal mercuric iodide, *Nucl. Instr. and Meth. A,* vol. 380, pp. 88-92, 1996.

[13] B. V. Shulgin. S. I. Gorkunova, V. L. Petrov, et al., Some scintillation properties of HgI_2 single crystal, *Proc. Int. Conf. On Inorganic Scintillators and Their Applications*, SCINT95, pp. 459-461 (Delft University Press, The Netherlands, 1996); *ibid*. pp. 469-471.

[14] R. Kleim and F. Raga, Exciton luminescence in lead iodide. Lifetime, intensity and spectral position dependence on temperature, *J. Phys. Chem. Solids*, vol. 30, pp. 2213-2223, 1969.

[15] S. Yamazaki and T. Goto, Stokes and anti-Stokes pair luminescence in PbI_2, *J. Phys. Soc. Jpn*., vol. 51, pp. 3228-3235, 1982.

[16] V. A. Bibik and N. A. Davydova, donor-acceptor emission in PbI_2 crystals, *Phys. Stat. Sol.(a)* 126, pp. K191-196, 1991

[17] Ch. Frick, U. Neukirch, R. Heitz, et al., Recombination kinetics of CdS:In, *J. Cryst. Growth*, 117, pp. 783-787, 1992.

[18] U. Neukirch, I. Broser, and R. Rass, Nonlinear luminescence of heavily doped CdS:in crystals, *Phys. Stat. Sol.(b)* vol. 159, pp. 431-436, 1990.

[19] M. Leroux, N. Grandjean, B. Beaumont, et al., Temperature quenching of photoluminescence intensities in undoped and doped GaN, *J. Appl. Phys*. vol. 86, pp. 3721-3728, 1999.

[20] M. Smith, G. D. Chen, J. Y. Lin, et al., "Mechanisms of band-edge emission in Mg-doped *p*-type GaN," *Appl Phys. Lett.,* vol. 68, pp. 1883-1885, 1996